# A Preliminary Study to Investigate Muscular Effects for Pedestrian Kinematics and Injuries Using Active THUMS

Masami Iwamoto, Yuko Nakahira

***Abstract*** Reduction in the number of pedestrian fatalities is one of the most significant issues in Japan. To address this issue, it is critical to estimate pedestrian kinematics, especially head impact locations during car-to-pedestrian impacts. In this study, we developed a pedestrian whole body finite element model with muscles which we call Active THUMS and validated the model with no activation against three series of human cadaver test data on quasi-static 3-point bending tests, shearing and bending impacts for pedestrian knees using two subjects and a SUV-to-pedestrian impact using one subject. The model was used for a preliminary study to investigate muscular effects on pedestrian kinematics and injuries, especially on the head-neck kinematics and brain injuries during SUV-to-pedestrian impacts. We hypothesized three types of activation levels of an assumed tensed condition, measured EMG data and only neck muscles from the literature. The comparison of simulation results with and without muscle activity showed that muscle activity altered pedestrian kinematics in the head and lower extremities and decreased skeletal injury risks and neck elongation. These findings partially correspond to differences in pedestrian injury patterns between cadaver test data and accident cases. Further studies are needed to estimate the muscle activation levels of pedestrians.

***Keywords*** Pedestrian accident, muscle activity, finite element model, kinematics, injury risk.

## I. INTRODUCTION

Recent Japanese traffic accident data show that the number of pedestrian fatalities is larger than that of occupant fatalities. The proportions of Japanese traffic accident fatalities in year 2011 were reported as 37% in pedestrians, 32% in cyclists and 31% in occupants. Therefore, reduction in numbers of pedestrian accidents and pedestrian victims is one of the most significant issues in Japan. Currently, active safety devices such as a driver warning or an Automatic Emergency Brake (AEB) system with some sensor systems of millimeter wave radar, stereo camera, near-infrared sensors and so on have been developed to decrease the number of pedestrian accidents while passive safety devices such as pop-up hood, pedestrian airbag and so on have been developed to reduce the severity of pedestrian injuries. Chauvel et al. [1] estimated that in the case of no system failures, the AEB for pedestrians with detection sensors of both radar and camera would reduce fatal pedestrian crashes by 15.3% and seriously injured pedestrian crashes by 38.2% each year in France based on French accident data. The active safety devices would be effective for reduction in pedestrian accidents, and fatal and serious injuries. However, they still have some limitations on unavoidable crashes due to higher speeds of striking vehicles and non-detection of struck pedestrians even in lower vehicular speeds, which could occur when the struck pedestrians are standing, walking or running in environments with other obstacles such as other vehicles. Therefore, passive safety devices still would be effective for mitigating pedestrian injury risks.

According to pedestrian accident data analysis using the CIREN (Crash Injury Research and Engineering Network) database performed by Mueller et al. [2], the most frequently injured body region was the head followed by the leg. Inomata et al. [3] developed a pop-up engine hood system for pedestrian head protection by creating space between the hood and the engine component, and confirmed that the system would reduce the HIC (Head Injury Criterion) by computer simulations using a mid-size adult human body finite element (FE) model. Jakobsson et al. [4] developed a pedestrian airbag system and showed that the airbag system would help reduce the head acceleration level when the head hit the area around the windscreen wiper recess and A-pillar by using pedestrian FE models of four different body sizes with three different stances. However, it is

M. Iwamoto is a senior researcher (tel: +81 (561) 71-8007, fax: +81 (561) 63-6459, iwamoto@mosk.tytlabs.co.jp) and Y. Nakahira is a researcher, both in Impact Mechanics Lab., Mechanical Engineering Dept. II, Toyota Central R&D Labs., Inc., Japan.

not easy to predict kinematics of pedestrians subjected to vehicular impacts because a variety of body sizes, stances and muscle activity has the potential to affect pedestrian kinematics. In particular, in their simulations, effects of muscle activity on pedestrian kinematics and injury outcomes were not considered. Recently some researchers demonstrated that muscle activity of occupants has significant effects on occupant kinematics and injuries, especially at low speed impacts [5-7]. Therefore, it is necessary to investigate how muscle activity of pedestrians who may be standing, walking, running and so on in the pre-crash phase of car-to-pedestrian impacts could affect their kinematics and injury outcomes.

The purpose of this study is to develop an FE model of a pedestrian including muscle activity, and investigate muscular effects on pedestrian kinematics and injury outcomes in traffic accidents. In our previous studies [7-8], we developed a human body FE model THUMS (Total HUman Model for Safety) with 3D geometry of muscles in the whole body, which we call Active THUMS. In this paper, we performed a preliminary study using Active THUMS to investigate effects of muscle activity on pedestrian kinematics and injuries, in particular, the effects of muscle activity on the head-neck kinematics and brain injuries. All simulations were performed by using an explicit finite element code LS-DYNA v971 Revision 3.2.1 (LSTC, USA).

## II. METHODS

### *Pedestrian FE model with multiple muscles*

In our previous studies [7-8], we developed a mid-size adult male occupant FE model with 3D geometry of muscles in the whole body, whose height and weight were 175 cm and 77 kg, respectively (Figure 1(a)). The model was created by integrating each muscle model in the human whole body with a human body FE model THUMS AM50 (Adult 50$^{th}$ percentile male) Version 1.4, which we developed previously. We call the model Active THUMS. Each muscle model of Active THUMS was represented by coupling bar elements to solid elements by shared nodes as shown in Figure 1(a). The bar elements can contract according to muscle activation level by using the Hill-type muscle model (LS-DYNA MAT156) while the solid elements molding the muscular 3D geometry can deform with incompressible hyper-elastic material properties by using a rubber-like material model (LS-DYNA MAT181). This modeling can represent muscular stiffness change according to the activation level [7] [9].

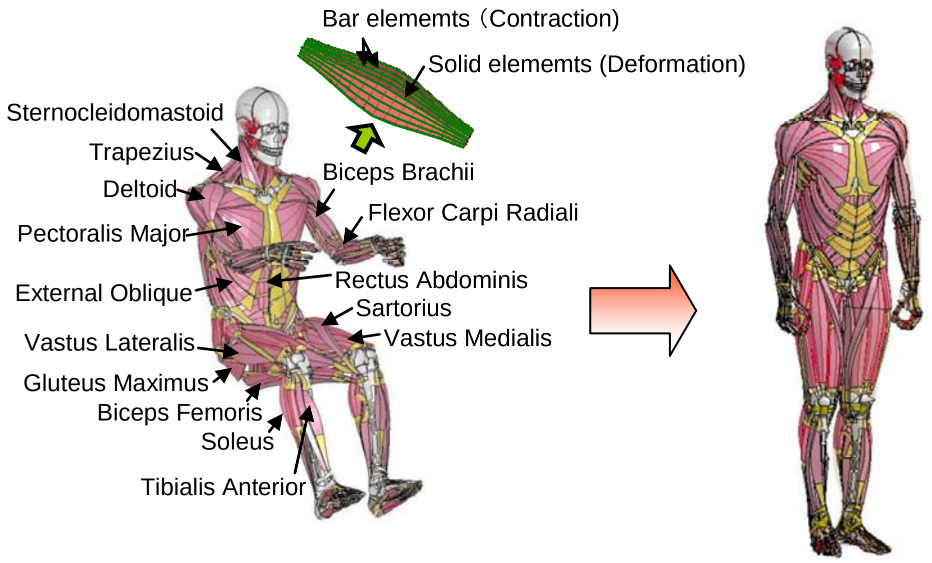


(a) Occupant FE model (b) Pedestrian FE model

Fig. 1. Occupant FE model and pedestrian FE model of Active THUMS.

The Active THUMS includes 282 muscles of lower extremities, upper extremities, trunk and neck such as the Sternocleidomastoid, Trapezius, Rectus Abdominis, Erector Spinae, Pectoralis Major, Deltoid, Biceps Brachii, Triceps, Extensor Digitorum, Rectus Femoris, Gluteus Maximus, Vastus Medialis, Biceps Femoris, Vastus Lateralis, Tibialis Anterior, Gastrocnemius and so on. Total numbers of elements and nodes in the whole body model were about 283,000 and about 151,000, respectively. A pedestrian FE model was developed by changing a sitting posture of the occupant FE model to a standing posture as shown in Figure 1 (b). The method to change the posture of the model can be found in the authors' paper [7]. In addition, the occupant FE model of Active THUMS without muscle activity was validated against several series of human cadaver test data on shoulder belt loadings for the thorax, lap belt loadings for the abdomen, head-neck responses during a frontal impact, and occupant kinematics and injuries during frontal impact sled tests [7]. On the other hand, the occupant FE model with muscle activity was validated against some volunteer test data on arm flexion kinematics, muscle stiffness change of the biceps brachii muscle, and the kinematics and mechanical responses of a driver in a bracing condition with pushing his hands on a handle and his right foot on a pedal [7].

***Validation of pedestrian FE model***

***Quasi-static 3-point bending tests of long bones in the lower extremity***

For validation of the pedestrian FE model, firstly cadaver test data on quasi-static 3-point bending tests of long bones in the lower extremity were used in this study to validate the model against mechanical responses of the lower extremities during car bumper-to-pedestrian leg impacts. Yamada [10] reported load-deflection curves in quasi-static 3-point bending tests of wet long bones obtained from human cadavers with ages ranging from 20 to 39 years. In these tests, the long bones were supported by plaster or concrete at bottom ends and then the center of the long bones was loaded to failure by the loading head of a testing machine in an antero-posteior direction. In this study, quasi-static 3-point bending simulations were performed to validate the model of the femur, tibia and fibula against the load-deflection properties. Each bone was fully fixed at the posterior ends and the center of each bone was compressed gradually at a constant velocity of 1.0 m/s to reproduce the test conditions. The load-deflection curves were compared between simulation results and test data.

***Shearing and bending impacts for knee joint***

Secondly, cadaver test data on shearing and bending impacts for the knee joint were used in this study to validate the model against kinematics and mechanical responses of the lower extremities during car-to-pedestrian impacts. Kajzer et al. [11] conducted a series of cadaver tests on shearing and bending impacts for a simulated pedestrian knee using ten fresh PMHS (Post Mortem Human Subject). According to Kajzer et al., each cadaver subject was lying supine on the stable table and the left thigh was fixed with two fixation devices including load cells on the distal part of the femur and the trochanter. The upper part of the table was movable and connected to a pneumatic system to achieve preload of the left lower extremity during experiments with a force of 400N to reproduce a force between a foot and the ground in a standing posture. An impactor including an accelerometer, a load cell and styrofoam, of which the total mass was 6.25 kg, was propelled by a spring at the lower part of the left knee joint in the shearing tests while the impactor was propelled at the right ankle joint in the bending tests. The initial velocity of the impactor used in their tests was 40 km/h. The simulation setups using the pedestrian FE model were determined to reproduce the above-mentioned experimental setups as shown in Figure 2. Although the whole body was used in the tests, the lower body, in which the sacrum and lumber spines were fixed, was used in the simulations. A preload of 400N was applied to the left foot in the shearing test and the right foot in the bending test before impact. An impactor weighing 6.25 kg was laterally impacted to the lower part of the left knee joint in the shearing test and to the right ankle joint in the bending test while the distal part of the femur and the trochanter were fixed with bar elements. In the shearing tests, impactor acceleration and Y-displacement of two target markers of P1 and P2 were obtained from simulation results and were compared with those from two subjects of the cadaver test data [12]. In the bending tests, knee bending moment, shearing displacement, and bending angle were

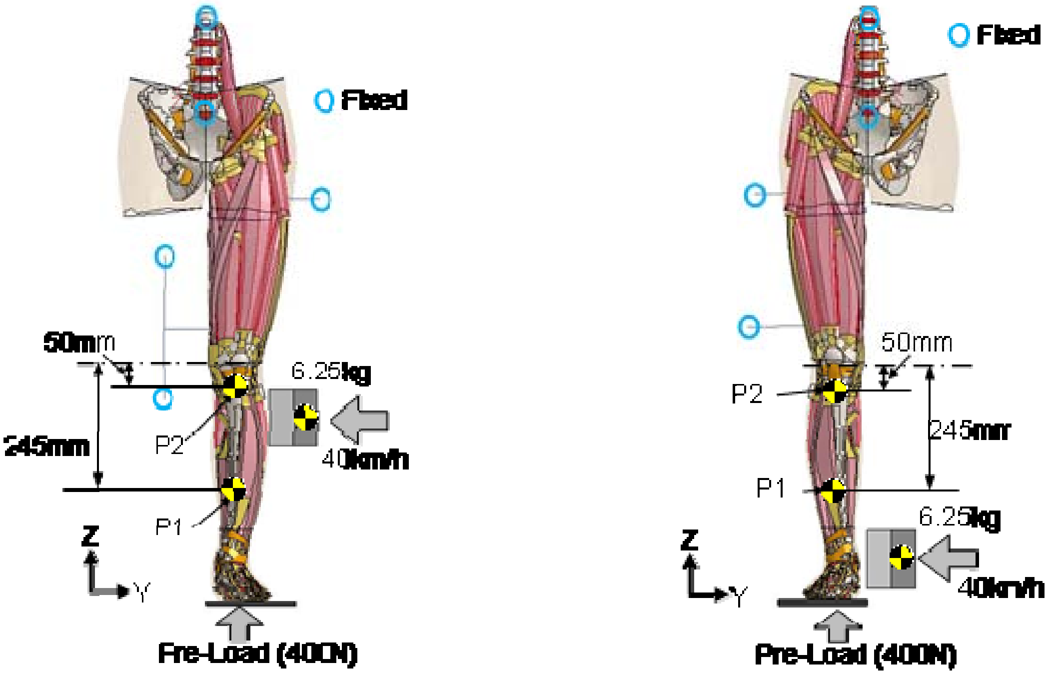


(a) Shearing impact (b) Bending impact

Fig. 2. Simulation setups of shearing and bending impacts for knee joints using the pedestrian FE model.

***Whole body kinematics***

Thirdly cadaver test data on whole body kinematics and injuries during car-to-pedestrian impacts were used in this study. Schroeder et al. [14] conducted a series of cadaver tests on whole body behaviors of pedestrians in colliding with a SUV (Sport Utility Vehicle) or a Mini-Van using four fresh PMHS. In this paper, only a validation for whole body behaviors and injuries of a pedestrian of one fresh PMHS in colliding with a SUV was described. In the cadaver tests conducted by Schroeder et al., a vehicle buck sled of a SUV was set to hit a cadaver in an upright standing posture laterally with an initial velocity of 40 km/h to simulate a typical car-to-pedestrian accident in which a pedestrian was crossing the road in front of a vehicle. The left leg of a cadaver was set forward while the right leg was set backward. The left knee was set in a position that it could collide with the center of the bumper. The bare feet without socks were set 25 mm above the ground level, which was considered as the height of an ordinary shoe. A steel wire was fixed with the head to maintain the upright standing posture until 60 ms before the beginning of the impact. The hands were bound with medical tape with low adhesion and were set in front of the abdomen in order to prevent the hands from entering between the car and the lower limbs. In addition, cushioning material was set at and around the point of fall to prevent injuries by second collisions between the cadaver and the ground. The vehicle dimension and mass of the SUV used in the test are shown in Table 1. In this study, one data set of test No.HJ2, in which height, weight and age of the subject were 185 cm, 85 kg and 84 years old, respectively, was selected for comparison of simulation results using the pedestrian FE model. In the cadaver test, the trajectories of the head, T1, T6, L5, right and left knees, and right and left ankles were obtained and some injuries were observed as shown in Table 2.

TABLE I

VEHICLE DIMENSION AND MASS OF SUV

| | | |
|---|---|---|
| Bumper height (Top) | (mm) | 658 |
| Bumper protrusion | (mm) | 163 |
| Hood leading edge | (mm) | 709 |
| Hood length | (mm) | 861 |
| Hood inclination | (degree) | 9 |
| Windshield inclination | (degree) | 38 |
| Vehicle body mass | (kg) | 810 |

TABLE 2

INJURY OUTCOMES IN A SUV-TO-PEDESTRIAN IMPACT TEST

| | |
|---|---|
| Left knee | Rupture of deep part of MCL, which is connected to the medial meniscus<br>ACL - avulsion of femoral insertion<br>MCL - avulsion of tibial insertion |
| Pelvis (left ring) | Anterior pelvic ring fracture of inferior pubic ramus<br>Anterior pelvic ring fracture of iliopubic eminence |
| Left hand | Abrasion on the hand |
| Left arm | Abrasion on the forearm |
| Rib | Fracture of 5$^{th}$ and 6$^{th}$ rib at the medio clavicular line; 120 mm from the center line of the sternum, 130mm from the center line of the sternum |
| Head | Contusion |

Figure 3 shows a simulation setup of SUV-to-pedestrian impacts. A vehicle FE model of SUV was created by referring to a SUV vehicle FE model, which has been developed by the National Crash Analysis Center (NCAC) of The George Washington University under a contract with the FHWA (Federal Highway Administration) and NHTSA (National Highway Traffic Safety Administration) of the US DOT (Department of Transportation). The total numbers of nodes and elements of the vehicle FE model were about 221,000 and about 233,000, respectively. The roof and doors of the vehicle model were modeled as rigid bodies because the parts would not have any contacts with the human body. The pedestrian FE model was set to reproduce the cadaver test setup so that the left leg was set forward while the right leg was set backward. The left knee was set in a position that it could collide with the center of the bumper. The simulation setup reproduced the experimental setup used in the tests by Schroeder et al. The vehicle FE model hit the pedestrian FE model laterally with an initial velocity of 40 km/h under a gravity of 9.8 m/s$^2$. The vertical (Z-direction) and horizontal (Y-direction) displacements of target markers of the head, T1, T6, L5, right and left knees, and right and left ankles and head velocity relative to the vehicle were obtained from simulation results and were compared with those of cadaver test data. Additionally, the injury locations predicted by the pedestrian FE model were also compared with those from the cadaver test data.

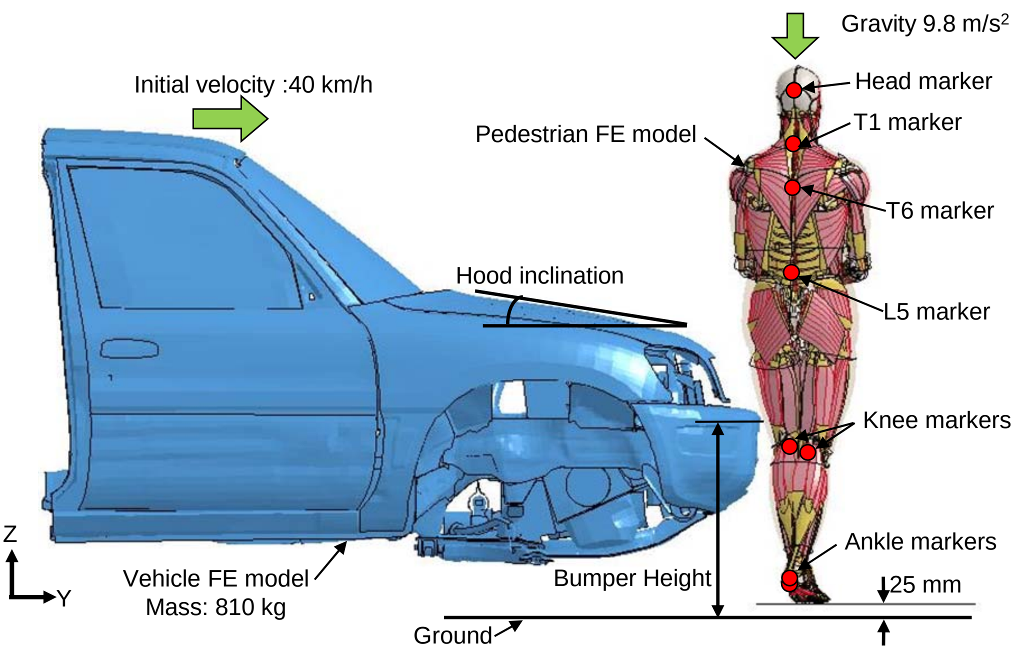


Fig. 3. Simulation setup of SUV-to-pedestrian impacts.

***An experimental test to investigate human muscle activations in a standing posture***

To investigate activation levels of some human muscles in a standing posture, a volunteer test was conducted in this study. A healthy male subject of 30 years old whose height and weight was 1.68 m and 72 kg, which were close to the size of AM50, without any history of neurological or musculoskeletal disorders participated in the volunteer test. He gave his informed consents. The procedures to measure the normalized muscle activation levels were approved by the institutional ethics committee and conducted in accordance with the Declaration of Helsinki. He held his posture on a standing posture with a normal psychological state, in which both knee joint angles were 175 degrees, right ankle joint angle was 102 degrees and left ankle joint angle was 109 degrees. The standing posture was close to that of Active THUMS seen in Figure 3. The EMG data of some muscles of the lower extremities and the trunk shown in Table 3 were measured using an EMG measurement system (MP150, Biopac systems, USA). A surface electrode was placed on each muscle. Processing of EMG signal was performed as follows. Firstly, full wave rectification was applied to each raw EMG signal, and then the obtained signals were filtered with second-order low-pass Butterworth filter with frequency of 2 Hz, and finally integrated rectified EMG (IEMG) was obtained. The muscle activation level of the subject was normalized by dividing the IEMG signal of each muscle measured in the test by the maximal EMG signal, which was obtained from other tests on the maximal voluntary force for each muscle. Table 3 also shows the obtained activation level of each muscle. The activation level of each muscle obtained from the EMG data was less than 5.05%.

TABLE 3
MUSCLE ACTIVATION LEVELS OBTAINED FROM EMG DATA

| Muscles | Activation level (%) |
|---|---|
| *Erector Spinae (Right)* | 3.62 |
| *Latissimus Dorsi (Right)* | 0.69 |
| *Trapezius (Right)* | 1.01 |
| *Rectus Abdominis (Right)* | 0.58 |
| *External Oblique (Right)* | 2.70 |
| *Rectus Abdominis (Left)* | 1.64 |
| *Gluteus Maximus (Right)* | 0.23 |
| *Biceps Femoris (Right)* | 0.20 |
| *Rectus Femoris (Right)* | 0.17 |
| *Gastrocnemius (Right)* | 0.76 |
| *Tibialis Anterior (Right)* | 0.24 |
| *Gluteus Maximus (Left)* | 0.53 |
| *Biceps Femoris (Left)* | 5.05 |
| *Rectus Femoris (Left)* | 0.75 |
| *Gastrocnemius (Left)* | 0.52 |
| *Tibialis Anterior (Left)* | 0.78 |

***Investigation of muscular effects using pedestrian FE model***

As a preliminary study to estimate muscular effects on pedestrian kinematics and injuries, two types of simulations with and without muscle activity were performed using the same simulation condition as the SUV-to-pedestrian impacts described above. In the case without muscle activity, activation level of each muscle should be set to 0.0 (0.0%), but it was set to values less than 0.01 (1.0%) to ensure computational stability. The pedestrian FE model without muscle activity corresponds to a cadaveric pedestrian and the simulation results without muscle activity are indicated as “No activation” in this paper. In the case with muscle activity, we hypothesized three types of activation levels based on available data of muscle activations for pedestrians because there are no data on muscle activations of a human body during pedestrian-to-vehicle impacts. Firstly, the activation levels of all agonists and antagonists of a pedestrian in a standing posture with a tensed psychological state were determined to be a constant value based on the hypothesis that a pedestrian in a standing posture with a tensed psychological state for an imminent vehicle could activate agonists and antagonists with the relatively higher activation level simultaneously. The constant value was set to 0.2 (20%), which was an average value of activation levels of trunk muscles or lower extremity muscles measured in volunteer tests on driver's bracing that authors conducted previously [7]. The simulation results with this type of activation levels are indicated as “Tensed” in this paper. Secondly, the activation levels of some muscles were determined based on EMG data measured from a volunteer subject in a standing posture with a normal psychological state described above. In this case, the muscle activation levels less than 5.05% listed in Table 3 were set based on the EMG data and the activation levels of the other muscles were set to values less than 0.01 (1.0%). The simulation results with this type of activation level are indicated as “EMG” in this paper. In these two kinds of activation levels, the activation level of each muscle was increased from 0.0 to 0.2 in the period of 200 ms before impact and then the activation level of 0.2 was maintained until the end of the simulations. Thirdly, the time histories of activation levels of some muscles only in the neck region were set to those shown in Alvarez et al. [15], in which the activation levels ranged from 30 to 100%. In this case, the muscle activation levels in the other regions except the neck region were set to values less than 0.01 (1.0%). The simulation results with this type of activation level are indicated as “Only Neck” in this paper.

Firstly, we performed overall investigation of muscular effects on pedestrian kinematics and injuries by parametric simulations with two different muscle activation levels in two different impact velocities. We performed simulations using the pedestrian FE model with two muscle activation levels of “No activation” and “Tensed” in two initial velocities of 40 km/h and 20 km/h. The vertical (Z-direction) and horizontal (Y-direction) displacements of target markers of the head, T1, T6, L5, right and left knees, and right and left ankles as well as whole body kinematics of pedestrians were obtained from simulation results and were compared. Contact forces between human body parts and the vehicle model, and the number of skeletal injuries in the whole body predicted by the pedestrian FE model were also compared.

Secondly, we performed the detailed investigation of muscular effects on the head kinematics and brain injuries of the pedestrian FE model by parametric simulations with four different muscle activation levels of “No activation”, “Tensed”, “EMG” and “Only Neck” in only an initial velocity of 40 km/h. This is because the brain injury is the primary cause of death in fatal pedestrian accidents and the occurrence of the brain injury could be significantly affected by head-neck motions with muscle activity during car-to-pedestrian impacts. For this investigation, we incorporated a human head/brain model of THUMS AM50 version 3.0, which we developed previously [16] into the pedestrian FE model to predict brain injury risks. Figure 4 shows a human head/brain model used in this study and one of the validation results of the head/brain model [16], which are comparisons of x-displacements of four brain markers during a head impact with peak linear acceleration of 200 $m/s^2$ and peak angular accelerations of 1860 $rad/s^2$ between simulation results using the head/brain model and cadaver test data of C755-T2 obtained from Hardy et al. [17]. The validation results demonstrate that the head/brain model has good biofidelity to simulate strain distributions of the brain tissue. Total numbers of elements and nodes in the pedestrian FE model with the head/brain model were about 308,000 and about 172,000, respectively. The vertical (Z-direction) and horizontal (Y-direction) displacements of target markers of the head, T1, T6, L5, left knees, and left ankles of the pedestrian model as well as the head resultant velocity were obtained from simulation results and were compared in the four simulations. Additionally, the neck elongation and two brain injury predictors, that is, the first principal strain and the CSDM (Cumulative Strain Damage Measure), were obtained from the simulation results and were compared in the four simulations. The neck elongation was assumed to be one of the neck injury mechanisms, and was used in the injury evaluations because Kerrigan et al. [18] reported from their video analysis of cadaver tests that relatively high elongation of the cervical spine was found in cases with neck injury when a whipping motion of the head and neck was observed after initial bumper/lower extremity contact and before head contact. The CSDM was proposed by Takhounts et al. [19] and used for evaluating DAI (Diffuse Axonal Injury), which is one of the brain injuries often seen in car-to-pedestrian accidents. The CSDM is defined as the percent volume of the brain that exceeds the specified first principle strain threshold. When the threshold of the first principal strain is set to 10%, the variable term is expressed as “CSDM 10%” in this study. Kimpara et al. [20] used the THUMS brain model under head translational and rotational accelerations obtained from 58 American Football game players including 25 concussions, and obtained injury risk curves for the maximum first principal strain and the CSDM 10%, 15%, 20%, 25%, 30% using logistic regression analyses. For 50% probabilities of concussions, their study proposed the maximum first principal strain and the CSDM 10% as 31.8 % and 18.2 vol%, respectively. Therefore, we used the two brain injury predictors of the maximum first principal strain and the CSDM 10% to compare the simulation results.

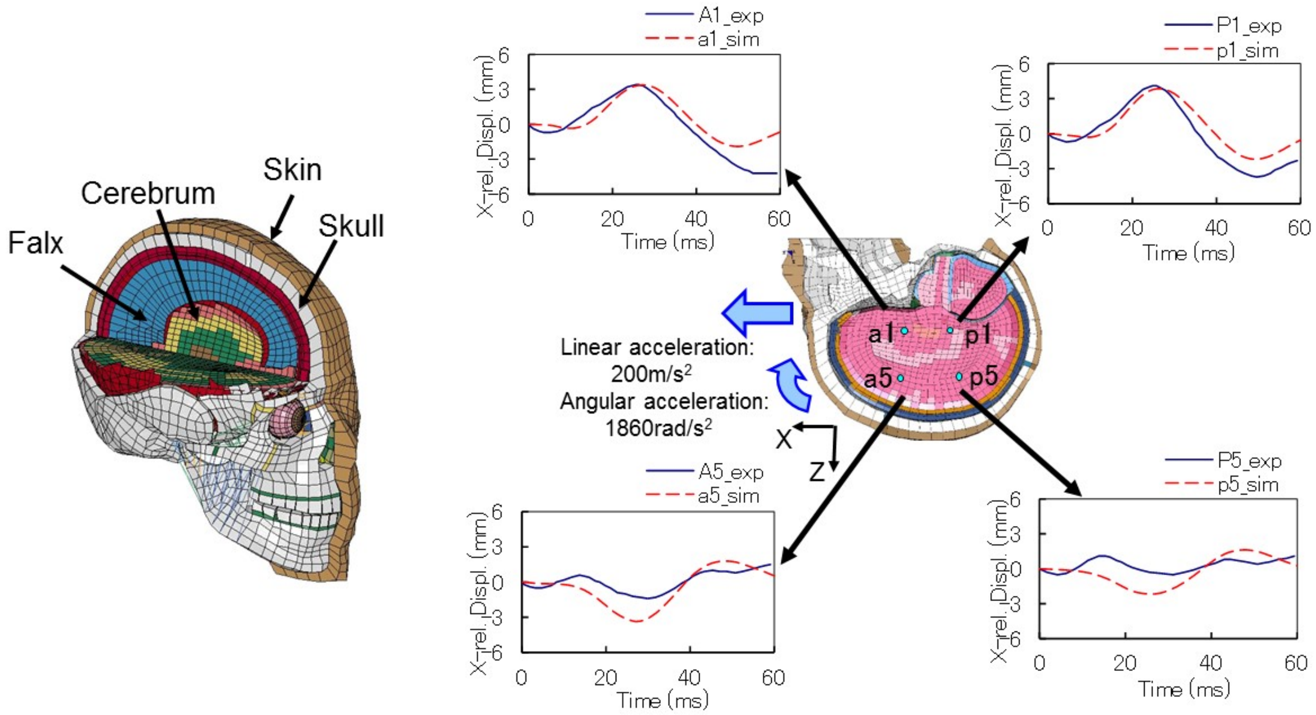


(a) Head/brain FE model (b) Comparison of x-displacements of brain markers during a head impact

Fig. 4. Head/brain FE model and its validation against a head impact with linear and angular accelerations.

## III. RESULTS

***Validation of pedestrian FE model***

***Quasi-static 3-point bending tests of long bones in the lower extremity***

Figure 5 shows comparisons of load-deflection curves in quasi-static 3-point bending tests of the femur, tibia and fibula between simulation results and test data. The load-deflection curve in each test was reported as an average value with ages ranging from 20 to 39 years [10]. Simulation results show good agreement with test data in the femur and tibia, although the failure strain predicted by the model was different from that obtained from the test data in the fibula.

***Shearing and bending impacts for knee joint***

Figure 6 shows comparisons of impactor acceleration, displacements of two target markers of P1 and P2 in the Y direction during a shearing impact with 40 km/h between simulation results and cadaver test data. The target markers of P1 and P2 were located at 245 mm and 50 mm below the center of the knee joint, respectively. Among the ten subjects, two tests Nos. 8S and 16S were selected from 40 km/h for the comparison, because the selected subjects were close to the pedestrian FE model in stature and weight and were without any bone fractures in fixed regions. As shown in Figure 6, impactor accelerations and the displacements of P1 and P2 predicted by the pedestrian FE model showed good agreement with those of test data. Therefore, the lower extremity of the pedestrian FE model has good biofidelity in the shearing impact from a car bumper.

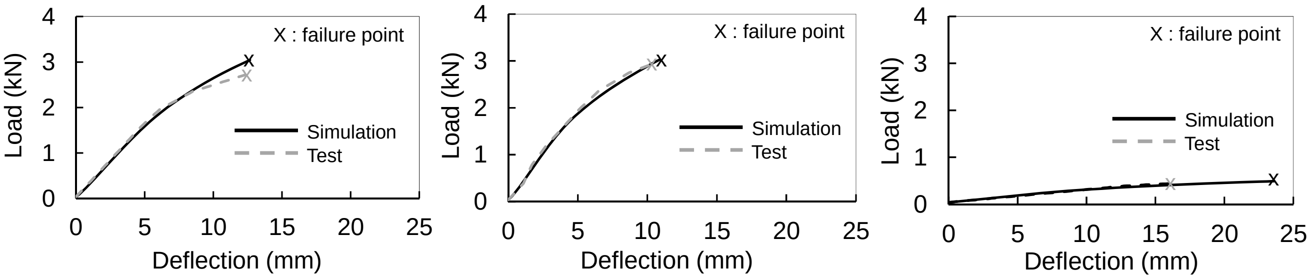


(a) Femur (b) Tibia (c) Fibula

Fig. 5. Load-deflection curves in quasi-static 3-point bending tests of the long bones in the lower extremity.

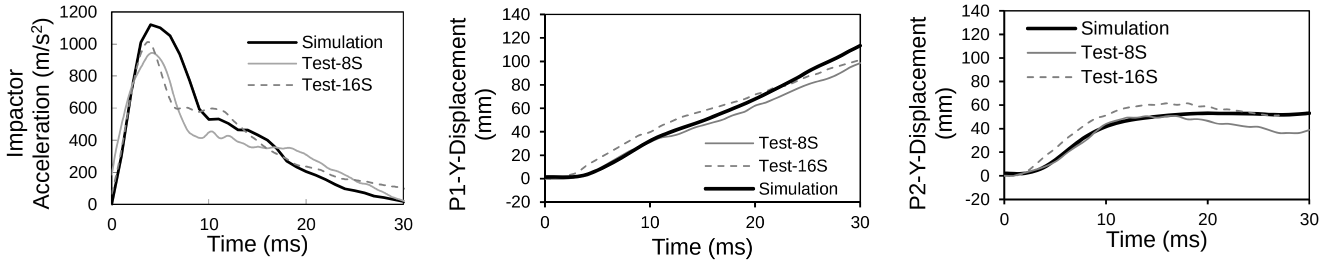


(a) Impactor acceleraion (b) Displacement of P1 (c) Displacement of P2

Fig. 6. Impactor accelerations and displacements of P1 and P2 in the Y direction during a shearing impact with 40 km/h.

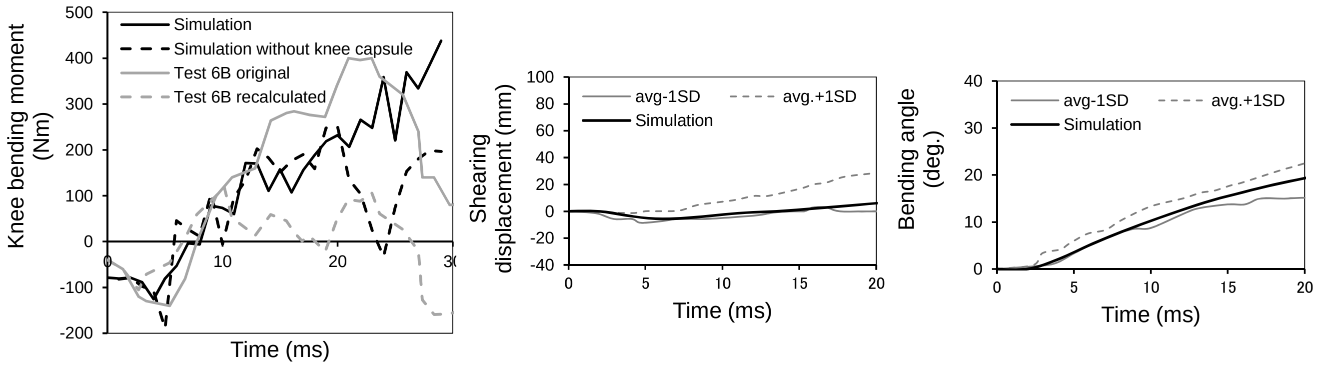


(a) Knee bending moment (b) Shearing displacement (c) Bending angle

Fig. 7. Knee bending moment, shearing displacement, and bending angle during a bending impact with 40km/h.

Figure 7 shows comparisons of knee bending moment, shearing displacement and bending angle during a bending impact with 40km/h between simulation results and cadaver test data. Konosu et al. [13] indicated that the knee bending moments calculated originally by Kajzer et al. [11] included an inadvertent calculation error that resulted in overestimation of the knee joint bending stiffness and injury tolerance. Therefore, in this study, the knee bending moment was recalculated according to Konosu et al. [13] and plotted on Figure 7(a). As shown in Figure 7(a), the knee bending moment predicted by the model was different from those obtained from the test data after 11 ms, although the predicted shearing displacement and bending angle fell within the test corridors reported by Konosu et al. [13]. In this study, we removed the knee capsule from the model and performed a simulation with the bending impact condition to investigate the cause of the inconsistency. The simulation result without the knee capsule is also included in Figure 7(a). The knee bending moment time history predicted by the model without the knee capsule seems to be similar to that of the recalculated test data, although the maximum bending moment is twice higher than the test data. Further study is needed to reproduce the knee bending moment during the bending impact by changing material properties of the knee capsule.

***Whole body kinematics***

Figure 8 shows a comparison of Y-Z displacements of target markers in the head, T1, T6, L5, right and left knees, and right and left ankles relative to the vehicle between simulation results with no activation and test data. The displacements of head, T1 and T6 predicted by the model showed good agreement with those obtained from the test data. However, the displacements of L5, knees and ankles were different between simulation results and test data after 80 ms. Figure 9 shows a comparison of head velocity relative to the vehicle between the simulation results with no activation and test data including test No.HJ1 in which the cadaver's height and weight are 165 cm and 60 kg, respectively. The simulation results agreed with the test data until 100 ms, but the head velocity predicted by the model decreased earlier in comparison with the test data after 100 ms. This is probably due to the difference in height between the model and the selected cadaver, because the simulation model with height of 175 cm is between HJ2 at 185 cm and HJ1 at 165 cm.

In this study, injury outcomes were also compared between the simulation results and test data. In the simulations, we found ACL (Anterior Cruciate Ligament) rupture in the left knee at 20 ms and PCL (Posterior Cruciate Ligament) rupture in the right knee at 30 ms. We also found bone fracture risks at left pelvic ring and four left ribs. Occurrence of ligament ruptures and bone fractures were determined by the element elimination method in which an element was eliminated when strain of the element exceeded the ultimate strain. In comparison with Table 2, injury outcomes predicted by the pedestrian FE model showed good agreement with cadaver test data, although some inconsistencies were seen; that is, PCL rupture was not found in cadaver tests while, in the simulation, MCL (Medial Collateral Ligament) rupture was not found and right tibia fracture risk was found.

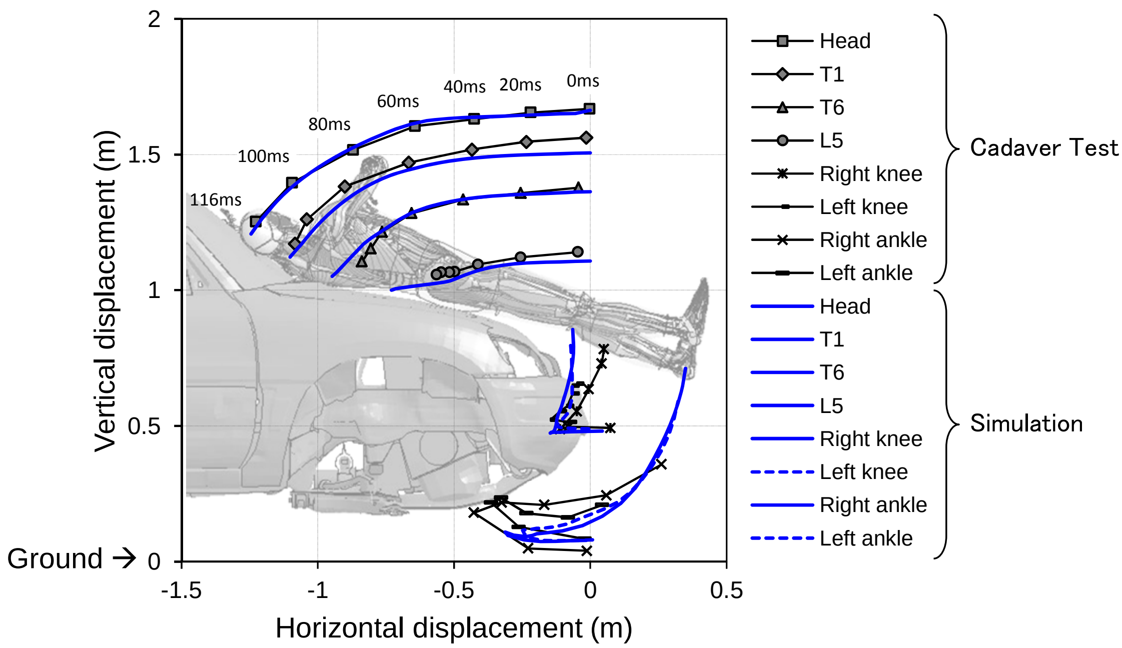


Fig. 8. Comparison of displacements of target markers in head, T1, T6, L5, knees and ankles between simulation results with no activation and cadaver test data.

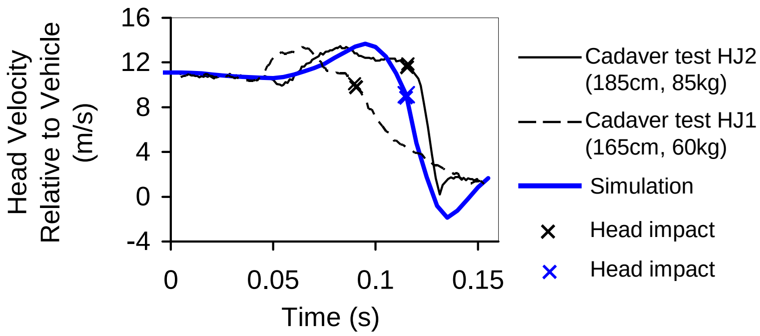


Fig. 9. Comparison of head velocity relative to the vehicle between simulation result with no activation and cadaver test data.

***Investigation of muscular effects using pedestrian FE model***

***Overall investigation of muscular effects on pedestrian kinematics and injuries***

Figure 10 shows comparisons of pedestrian kinematics during SUV-to-pedestrian impacts between four simulation cases of the two activation levels of “No activation” and “Tensed” in the two initial velocities of 40 km/h and 20 km/h. Figure 11 shows comparisons of Y-Z displacements of target markers in the head, T1, T6, L5, right and left knees, and right and left ankles relative to the vehicle between simulation results of “No activation” and “Tensed” in 40 km/h and 20 km/h. As shown in Figure 11(a), the pedestrian kinematics of “Tensed” were different from those of “No activation”, especially in contact locations of the head and upper bodies and motions of the lower extremities in 40 km/h. This is probably because the agonists and antagonists worked simultaneously in the case of “Tensed” so that they made each joint of the human body stiffer. As shown in Figure 11(b), the pedestrian kinematics were almost the same in the head and upper body between the cases of “No activation and “Tensed”, but were different in motions of the lower extremities in 20 km/h. Figures 12 and 13 show contact forces between human body parts and the vehicle model in 40 km/h and 20 km/h, respectively. In the case of “Tensed”, contact forces in the lower extremities were higher than in the case of “No activation” in both 40 km/h and 20 km/h. On the other hand, the head contact force was almost the same between the cases of “No activation” and “Tensed” in both 40 km/h and 20 km/h. Injury outcomes were also compared between simulation results of “No activation” and “Tensed” in both velocities of 40 km/h and 20 km/h. As shown in Table 4, the injury risks of knee ligament ruptures and rib fractures seem to decrease in the case of “Tensed” and in the lower velocity of 20 km/h.

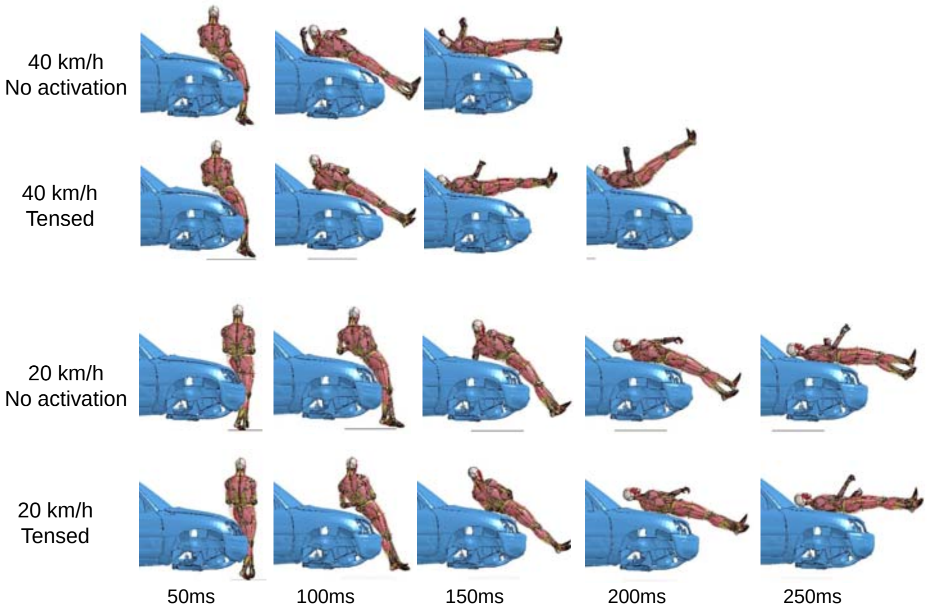


Fig. 10. Comparison of pedestrian kinematics during SUV-to-pedestrian impacts with low and high speeds.

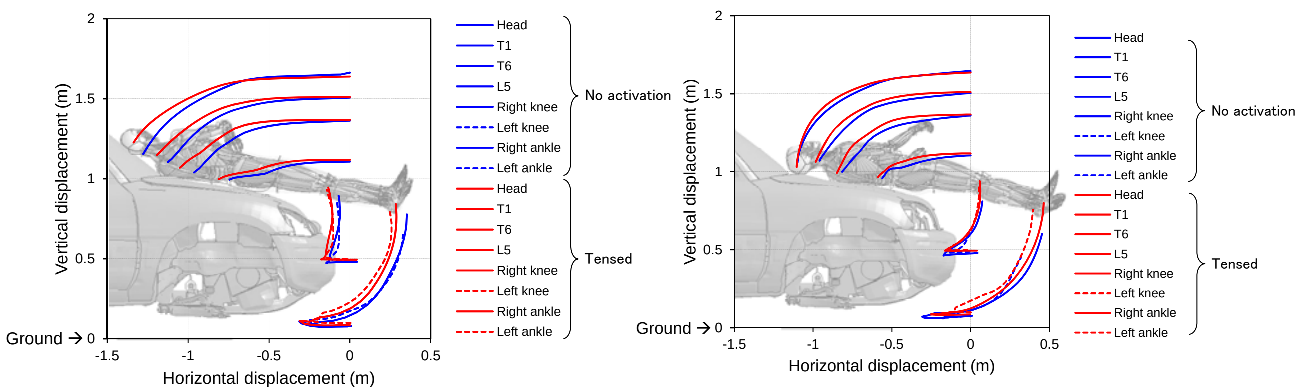


(a) 40 km/h (b) 20 km/h

Fig. 11. Comparison of displacements of target markers in head, T1, T6, L5, knees and ankles between simulation results of “No activation” and “Tensed”.

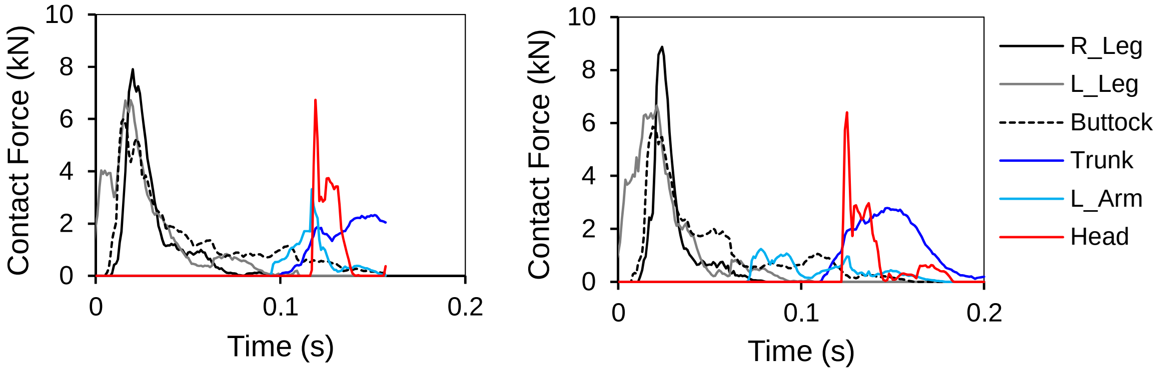


(a) No activation (b) Tensed

Fig. 12. Comparison of contact forces between human body parts and the vehicle model in 40 km/h.

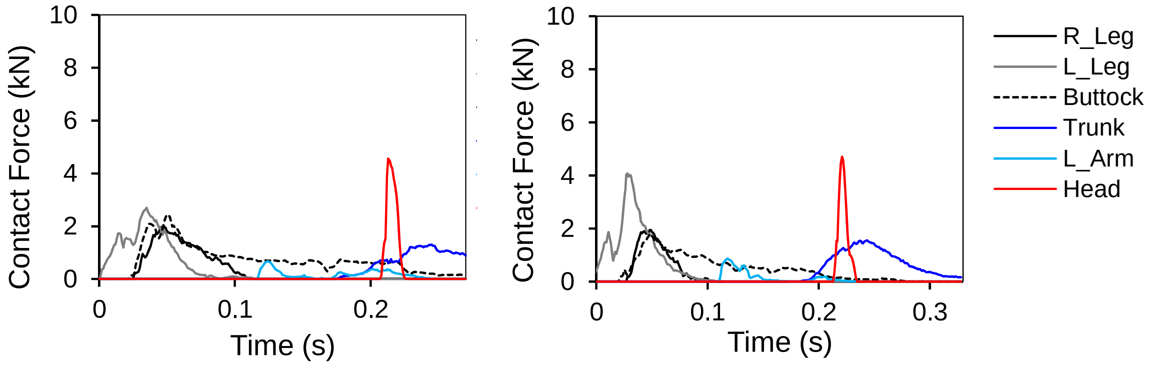


(a) No activation (b) Tensed

Fig. 13. Comparison of contact forces between human body parts and the vehicle model in 20 km/h.

TABLE 4

THE NUMBER OF INJURIES PREDICTED BY SIMULATIONS

| Injury types | No activation (40 km/h) | Tensed (40 km/h) | No activation (20 km/h) | Tensed (20 km/h) |
|---|---|---|---|---|
| *Knee ligament rupture* | 2 | 1 | 0 | 0 |
| *Pelvis fracture* | 1 | 1 | 0 | 0 |
| *Rib fracture* | 4 | 2 | 2 | 1 |
| *Skull fracture* | 0 | 0 | 0 | 0 |

***Detailed investigation of muscular effects on pedestrian kinematics and injuries***

Figure 14 compares the pedestrian kinematics of the head, T1, T6, L5, left knees and left ankles relative to the vehicle among four types of muscle activation levels in 40 km/h. For the kinematics of the ankle joint, the two cases of “EMG” and “Only Neck” were almost the same and were between the case of “No activation” and the case of “Tensed”. For the head kinematics, the case of “EMG” was close to the case of “Tensed” while the case of “Only Neck” was close to the case of “No activation”. Figure 15 shows comparisons of head resultant velocity relative to the vehicle among the four types of muscle activation levels. The head resultant velocities were almost the same in three cases except the case of “Only Neck”, although the timings of head impact in the cases of “Tensed” and “EMG” were delayed from that in the case of “No activation” by 5ms. This is one of the reasons that the head kinematics in the cases of “Tensed” and “EMG” were different from those in the cases of “No activation” and “Only Neck” as described above. Figure 16 shows time histories of neck elongation among the four cases. The neck elongation was calculated as different from the initial length between the posterior part of T1 spinous process and the posterior atlanto-occipital membrane. Before impact, the head and neck had a compression in the cases of "Tensed" and "Only Neck". The maximum neck elongations in the cases of "No activation", "Tensed", "EMG" and "Only Neck" were 39.0, 32.5, 41.3, and 5.2 mm, respectively. Therefore, muscle activations in the neck seem to decrease the neck elongation. Figure 17 compares the maximum values of the brain injury predictors among various types of muscle activation levels in 40 km/h. As shown in Figure 17, both brain injury predictors obtained from all four simulation results exceeded their thresholds proposed by Kimpara et al. [20]. These results indicate that in all four simulation cases, the pedestrian FE model had the potential to sustain mild traumatic brain injury.

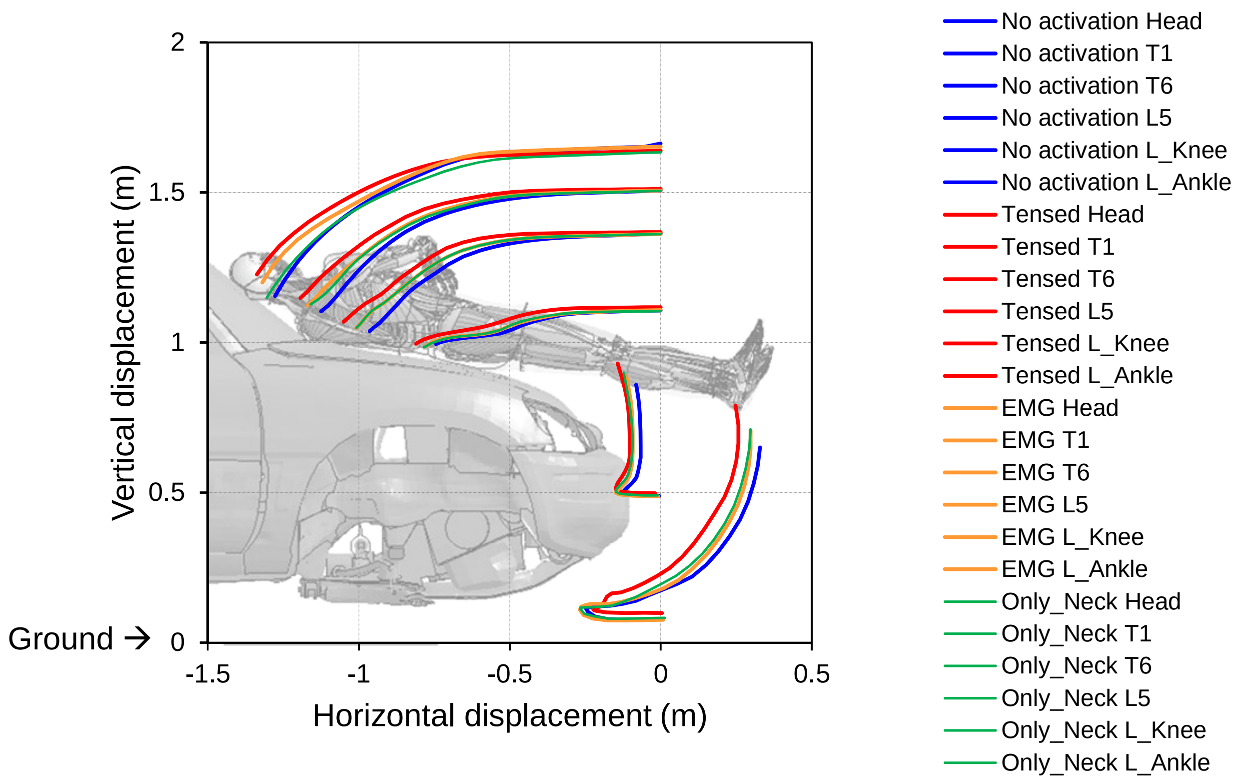


Fig. 14. Comparison of displacements of target markers in head, T1, T6, L5, knees and ankles between simulation results with various types of muscle activity in 40 km/h.

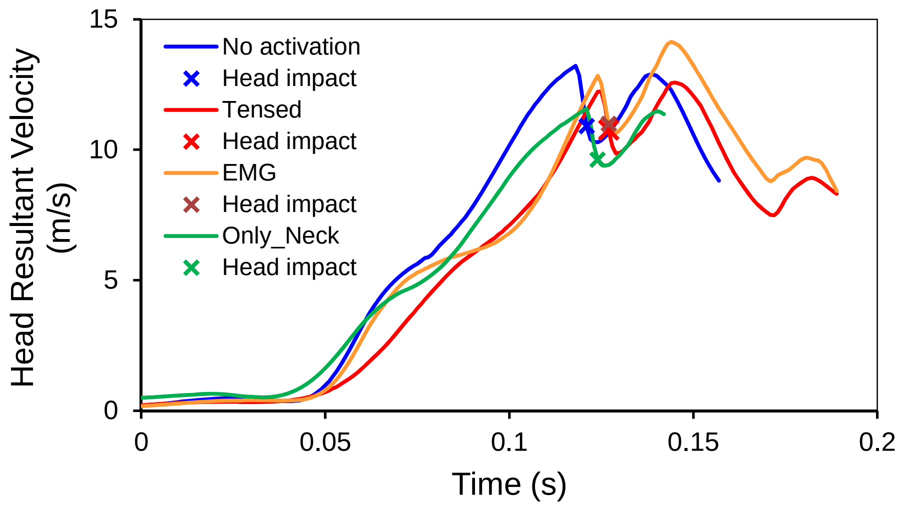


Fig. 15. Comparison of head resultant velocity relative to vehicle among various types of muscle activations in 40 km/h.

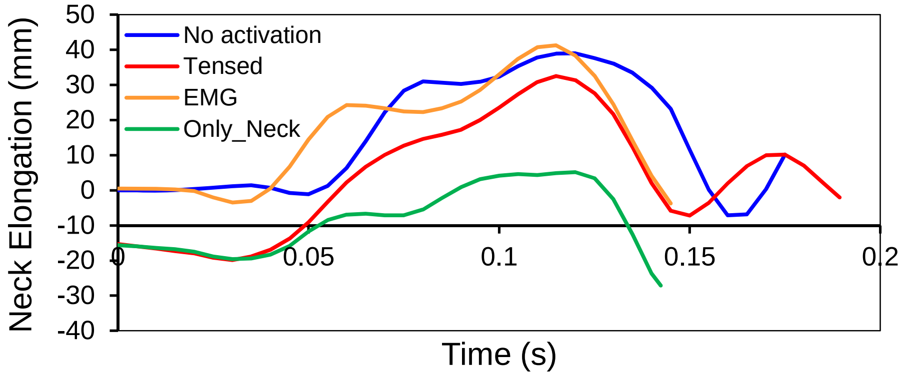


Fig. 16. Comparison of neck elongation time histories among various types of muscle activations in 40 km/h.

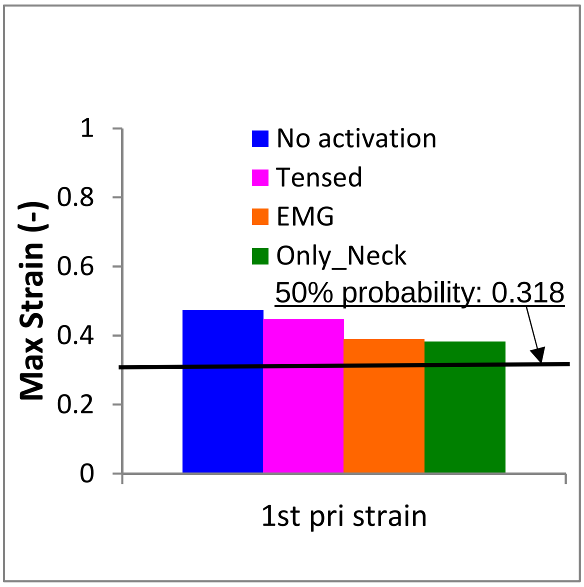


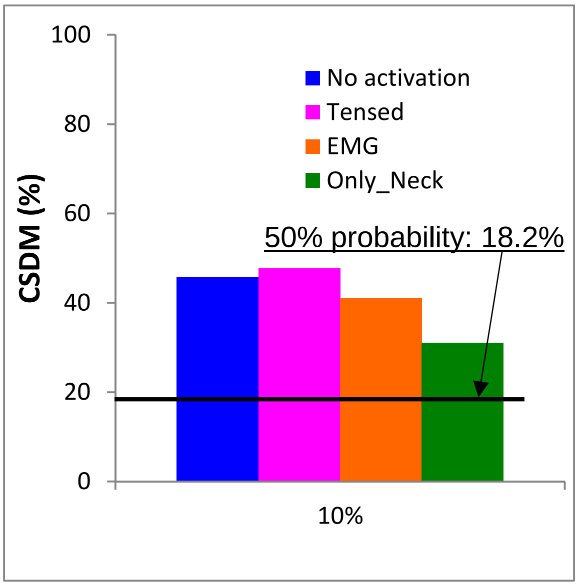


(a) Maximum first principal strain (b) CSDM 10%

Fig. 17. Comparison of maximum values of brain injury predictors among various types of muscle activation in 40 km/h

## IV. Discussion

In this study, we developed a pedestrian FE model with muscles and validated the model with no activation against three series of cadaver test data on quasi-static 3-point bending tests, shearing and bending impacts for the knee joint, and whole body kinematics and injuries during SUV-to-pedestrian impacts. After we confirmed that the pedestrian FE model with no activation had almost the same biofidelity as cadavers, we performed a preliminary study using the pedestrian FE model to investigate effects of muscle activity on pedestrian kinematics and injuries. Since there are no data on muscle activations of a human body during pedestrian-to-vehicle impacts, we hypothesized three types of activation levels as “Tensed”, “EMG” and “Only Neck” based on available data of muscle activations for pedestrians. From the simulation results on the overall investigation of muscular effects with the two activation levels of “No activation” and “Tensed”, the muscle activity showed effects on impact locations of the head and upper body in only 40 km/h while the muscle activity showed effects on motions of the lower extremities in both 40 km/h and 20 km/h because the muscle activity made each joint of the lower extremities stiffer and caused higher contact forces of the lower extremities in the case of “Tensed”. The reason why the head contact force was almost the same between the cases of “No activation” and “Tensed”, although the head contact locations were different between the two cases in 40 km/h as shown in Figures 11(a) and 12, is because the head velocity of “No activation” was almost the same as that of “Tensed” in the timing of head impact as shown in Figure 15 as well as the material properties and geometry of windshield where the head hit were the same in the two cases. From the simulation results on the detailed investigation of muscular effects with four activation levels of “No activation”, “Tensed”, “EMG” and “Only Neck”, as shown in Figure 14, the muscle activity in the trunk and the lower extremities showed some effects on the head impact locations, because the cases of “Tensed” and “EMG” included muscle activation levels of 20% and less than 5.05%, respectively, in the trunk and the lower extremities while the cases of “No activation” and “Only Neck” included muscle activation levels of less than 1.0% in the trunk and the lower extremities. Figures 14 and 15 suggest that the muscle activity in the trunk and the lower extremities could delay the timing of head impact. Therefore, the muscle activity in the trunk and the lower extremities could have significant influence on the timing and location of head impact. From Figure 16, the higher activation levels in the neck muscles tend to decrease the neck elongation, because the cases of “Tensed” and “Only Neck” included muscle activation levels of 20% and 30-100%, respectively, in the neck while the cases of “No activation” and “EMG” included activation levels of less than 1.0% in the neck. The activation levels used in the case of “Only Neck” are the same as those used in a pedestrian FE model developed by Alvarez et al. [15]. They also investigated the effect of the neck muscle tonus on head kinematics in pedestrian-to-car collisions by FE simulations. They used a human body FE model THUMS version 1.4 with neck muscles modeled as discrete springs with passive and active properties, in which active properties were modeled with Hill-type muscle contraction. They concluded that the neck muscle tonus showed an influence on the head impact angles. They showed the head resultant linear accelerations of their simulation results with passive muscles and startle muscle tonus in the simulation condition of an initial velocity of 40 km/h and a posture of struck leg forward were 350 and 340 g, respectively. They also showed that the head resultant angular accelerations of their simulation results with passive muscles and startle muscle tonus in the same simulation condition were 20 and 25 krad/s$^2$, respectively. In our study, the head resultant linear accelerations of simulation results of “No activation”, “Tensed”, “EMG” and “Only Neck” were 160, 187, 160 and 145 g, respectively. The head resultant angular accelerations of simulation results of “No activation”, “Tensed”, “EMG” and “Only Neck” were 12.3, 9.3, 11.7 and 10.3 krad/s$^2$, respectively. The tendency of the head resultant linear accelerations obtained in this study was the same as that reported by Alvarez et al. while the tendency of the head resultant angular accelerations obtained in this study was different from that reported by them. This inconsistency is probably due to the different muscle modeling technique between our muscle models including both bar elements and solid elements and their muscle model including only bar elements. From simulation results obtained in this study, the muscle activity in the neck had a tendency to decrease the head resultant linear and angular accelerations, although the constant activation levels of 20% for all muscles in the case of “Tensed” increased the head resultant linear acceleration. Further study is needed to investigate effect of activation level in each muscle of the whole body on the kinematics of the head during car-to-pedestrian impacts.

In the simulation results on the overall investigation of muscular effects with two activation levels of “No activation” and “Tensed”, injury outcomes predicted by the pedestrian FE model were also compared. As a result, the injury risks tend to decrease in the cases with muscle activity and with the lower velocity of 20 km/h. Kerrigan et al. [18] compared injury outcomes of their vehicle-pedestrian impact tests using 17 PMHS and other researchers' tests using 24 PMHS with those of 67 US vehicle-pedestrian crash cases between 2002 and 2007 obtained from the CIREN pedestrian database. All PMHS tests were conducted with vehicular velocity of about 40 km/h while half of the estimated vehicle impact speeds in 24 accident cases with sufficient information were between 40 km/h and 55 km/h, with one case estimated to be below 40 km/h and 11 cases estimated to be 56 km/h or above. From their comparison study, Kerrigan et al. concluded that the PMHS tests resulted in greater frequency and severity of spinal injuries, pelvic injuries and knee injuries than in the accident cases, and the biggest discrepancy between injuries sustained by the PMHS and the CIREN pedestrian was injuries to the spine, especially the cervical spine. They explained that one potential source of cervical spine injury was extension of the neck and, in accident cases, the severe extension or tension of the neck was restricted by the active musculature that is absent in PMHS. They also explained that the discrepancy in the incidence of knee injuries was due to muscular support of the knee joint in walking/running/standing pedestrians in accident cases. As shown in Table 4, simulation results indicate that the muscle activation tends to decrease knee injury risk, which agrees with the explanation by Kerrigan et al., although there is no clear muscular effect in the pelvis injury risk.

In the simulation results on the detailed investigation of muscular effects with four activation levels of “No activation”, “Tensed”, “EMG” and “Only Neck”, as shown in Figure 16, muscle activation tends to decrease neck elongations, which also agrees with the explanation by Kerrigan et al. Therefore, consideration of muscle activation has the potential to explain the differences in injury outcomes between PHMS tests and accident cases. The two brain injury predictors of the first principal strain and the CSDM 10% exceeded their thresholds in all cases of muscle activations. The CSDM 10% of "Only Neck" was the smallest among the four cases. This might be explained by the fact that the head resultant velocity of "Only Neck" at the timing of head impact was the lowest among the four cases. This suggests that the muscle activity in the neck has a possibility to reduce the brain injury. However, the thresholds were determined by using mild traumatic brain injury data obtained from American Football game players, and the brain injury predictors used in this study are not sufficiently validated against biological data of human brain tissue yet. Therefore, further studies are needed to obtain the thresholds of severe traumatic brain injuries in traffic accidents and find more reliable brain injury predictors.

This study has some limitations on exclusion of simulations with other sizes of vehicles and pedestrians as well as on the model validation against pedestrians with muscle activations. In addition, the activation level of each muscle was set to a constant value before and after impacts. However, the muscle activation level could change with the time in the real human body. Further studies are needed to estimate activation level of each muscle in pedestrians who may be standing, walking, running and so on by some kinds of muscle controllers in the pre- and post-crash phases of various accident situations in order to reconstruct pedestrian injuries.

## V. CONCLUSIONS

Accurate estimation of pedestrian kinematics, especially head impact locations during car-to-pedestrian impacts, is critical for more reduction in the number of pedestrian fatalities. In this study, a pedestrian whole body FE model with a consideration of muscle activity was used for a preliminary study to investigate muscular effects on pedestrian kinematics and injury outcomes during SUV-to-pedestrian impacts. For consideration of muscle activity, we hypothesized four types of activation levels from the literature; that is, no activation, activation levels of an assumed tensed condition, those based on EMG data and those of only neck muscles. The comparison of the simulation results showed that the muscle activity in the trunk and the lower extremities could have significant influence on the timing and location of head impact while the muscle activity in the neck could have significant influence on the decrease of the neck elongation and the resultant linear and angular acceleration of the head. Additionally, the comparison showed that the muscle activity could decrease the skeletal injury risks of knee ligament ruptures and rib fractures, and neck injury risks with the neck elongation. These findings partially correspond to differences in pedestrian injury patterns between PMHS test data and CIREN pedestrian accident cases reported in the literature. Further studies are needed to estimate the muscle activation level of each muscle of pedestrians in the pre- and post-crash phases of various accident situations.

## VI. REFERENCES


[1] Chauvel C, Page Y, Fildes B, Lahausse J. Automatic emergency braking for pedestrians effective target population and expected safety benefits. *Proceedings of ESV Conference*, 2013, Seoul (Korea).

[2] Mueller BC, Nolan JM, Zuby DS, Rizzo AG. Pedestrian injury patterns in the United States and relevance to GTR. *Proceedings of IRCOBI Conference*, 2012, Dublin (Ireland).

[3] Inomata Y, Iwai N, Maeda Y, Kobayashi S, Okuyama H, Takahashi N. Development of the pop-up engine hood for pedestrian head protection. *Proceedings of ESV Conference*, 2009, Stuttgart (Germany).

[4] Jakobsson L, Broberg T, Karlsson A, Graberg N, Gullander C, Lindman M. Pedestrian airbag technology - A production system. *Proceedings of ESV Conference*, 2013, Seoul (Korea).

[5] Östh J, Brolin K, Carlsson S, Wismans J, Davidsson J. The occupant response to autonomous braking: A modeling approach that accounts for active musculature. *Traffic Injury Prevention*, 2012, 13(3):265-277.

[6] Meijer R, van Hassel E, Broos J, Elrofai H, van Rooij L, van Hooijdonk P. Development of a multi-body human model that predicts active and passive human behavior. *Proceedings of IRCOBI Conference*, 2012, Dublin (Ireland).

[7] Iwamoto M, Nakahira Y, Kimpara H, Sugiyama T, Min K. Development of a human body finite element model with multiple muscles and their controller for estimating occupant motions and impact responses in frontal crash situations. *Stapp Car Crash Journal*, 2012, 56:231-268.

[8] Iwamoto M, Nakahira Y, Sugiyama T. Investigation of pre-impact bracing effects for injury outcome using an active human FE model with 3D geometry of muscles. *Proceedings of ESV Conference*, 2011, Washington D.C. (United Sates).

[9] Iwamoto M, Nakahira Y, Kimpara H, Sugiyama T. Development of a human FE model with 3-D geometry of muscles and lateral impact analysis for the arm with muscle activity. *SAE Tech. Paper*, 2009, 2009-01-2266.

[10] Yamada H. Strength of Biological Materials, Williams & Wilkins Company, 1970.

[11] Kajzer J, Schroeder G, Ishikawa H, Matsui Y, Bosch U. Shearing and bending effects at the knee joint at high speed lateral loading. *SAE Tech. Paper*, 1997, 973326:151-165.

[12] Nagasaka K, Mizuno K, Tanaka E, Yamamoto S, Iwamoto M, Miki K, Kajzer J. Finite Element Analysis of Knee Injury Risks in Car-to-Pedestrian Impacts. *Traffic Injury Prevention*, 2003, 4:345-354.

[13] Konosu A, Issiki T, Tanahashi M. Development of a Biofidelic Flexible Pedestrian Leg-form Impactor (Flex-PLI 2004) and Evaluation of its Biofidelity at the Component Level and at the Assembly Level, *SAE Tech. Paper*, 2005, 2005-01-1879.

[14] Schroeder G, Fukuyama K, Yamazaki K, Kamiji K, Yasuki T. Injury mechanism of pedestrians impact test with a sport-utility vehicle and mini-van. *Proceedings of IRCOBI Conference*, 2008, Bern (Switzerland).

[15] Alvarez V, Fahlstedt M, Halldin P, Kleiven S. Importance of neck muscle tonus in head kinematics during pedestrian accidents. *Proceedings of IRCOBI Conference*, 2013, Gothenburg (Sweden).

[16] Kimpara H, Nakahira Y, Iwamoto M, Miki K, Ichihara K, Kawano S, Taguchi T. Investigation of Anteroposterior Head-Neck Responses during Severe Frontal Impacts Using a Brain-Spinal Cord Complex FE Model. *Stapp Car Crash Journal*, 2006, 50:509-544.

[17] Hardy WN, Foster CD, Mason MJ, Yang KH, King AI. Investigation of Head Injury Mechanisms Using Neutral Density Technology and High-Speed Biplanar X-Ray, *Stapp Car Crash Journal*, 2001, 45:337-368.

[18] Kerrigan JR, Arregui-Dalmases C, Foster J, Crandall JR, Rizzo A. Pedestrian injury analysis: field data vs. laboratory experiments, *Proceedings of IRCOBI Conference*, 2012, Dublin (Ireland).

[19] Takhounts EG, Crandall JR, Darvish K. On the Development of the SIMon Finite Element Head Model. *Stapp Car Crash Journal*, 2003, 47:107-133.

[20] Kimpara H, Iwamoto M. Mild Traumatic Brain Injury Predictors based on Angular Accelerations during Impacts, *Annals of Biomedical Engineering*, 2012, 40(1): 114-126.